Proceedings of the 21st ICSMGE, Vienna, Austria, 14 – 19 June 2026. Pistrol, Adam & Schweiger (eds.)
Published by: ÖGG, Austrian Society for Geomechanics, Salzburg, Austria, ISBN 978-3-9503898-4-5
https://doi.org/10.53243/ICSMGE2026-498

Effect of Geogrid Structure on Performance of Unpaved Roadways

Ghada Ellithy, Munibhaskar Pagadala
Dept of Civil Engineering, Embry Riddle Aeronautical University, Daytona Beach, Florida, USA, ellithyg@erau.edu.

ABSTRACT**:** This paper investigates the influence of geogrid structure, physical and mechanical properties on the performance of unpaved roadways. Geogrids are widely utilized as reinforcement materials in unpaved roadway construction, aiming to stabilize the subgrade, reduce rutting, and prolong service life. The objective of the research presented in the paper is to assess the effect of the structure of three geogrids on resilient modulus, resilient and plastic strain using cyclic triaxial testing. Three types of geogrids, characterized by varying aperture size, geometry and mechanical properties are compared to unreinforced section. To achieve this goal, a total of 12 cyclic triaxial tests were conducted on both unreinforced and reinforced samples. Each specimen is 150 mm in diameter and stands 300 mm tall. The lower segment integrates a blend of clay and sand materials to represent the subgrade, while the upper segment comprises aggregate material to represent the base course. A geogrid sample with the same diameter is cut and placed between the two materials. The base course thickness selected for this testing is 50 mm, while the subgrade is 250 mm and varies in strength of California Bearing Ratio (CBR) values of 1%, 2% and 4%. Each test was performed at 10,000+ cycles with different loading sequences per AASHTO 307 standard. Examining the three reinforced samples against the control (unreinforced) sample, several factors including, integrity of the geogrid structure, dimensional and mechanical properties and interlocking with the base aggregate are discussed in relation to the improvement in samples performance

KEYWORDS: Geogrids, cyclic triaxial, unpaved roadways,

1 INTRODUCTION AND BACKGROUND

In civil engineering, geogrids have become highly adaptable and are widely used to improve the longevity and performance of both paved and unpaved roads. Their use in road construction techniques has been crucial in addressing many transportation infrastructure-related issues, including deformation under severe loads, rutting, and structural instability. In this paper, we utilize cyclic triaxial testing to improve design and measure performance. It has been established that geogrids offer improvement in pavement performance through lateral stability and prevention of lateral movement of the base layer, which helps maintain the integrity of the overall structure. Geogrids also enhance the load-bearing capacity of the subgrade by distributing the loads over a larger area and provide tensile support preventing cracking or deformation. Research on geosynthetics in geotechnical and pavement engineering has significantly advanced, revealing their effectiveness in various scenarios and quantifying the geogrid reinforcement mechanisms, Ellithy and Crippa, 2023.

Studies by Wang et al. (2013), and Ziaie et al. (2018) highlighted how geotextile layers and initial shear stress affect soil behavior under cyclic loads, emphasizing the need to enhance soil response to such stressors. Further research by Kiptoo et al. (2017) and AL Sa'adi et al. (2022) showed the positive impact of geosynthetics on pavement construction, specifically in improving bearing capacity, settlement reduction, and rutting resistance. Salama et al. (2023) and Singh K et al. (2021) focused on geogrid reinforcement in unpaved roads and developing rutting prediction models, illustrating the importance of understanding material behavior under repeated stress. This research builds on these findings, aiming to explore the effectiveness of geogrid reinforcement in unpaved roads under cyclic triaxial tests of composite section. Composite sections feature a lower layer of bentonite clay and sand to mimic the subgrade and an upper aggregate layer as the base, which is essential for assessing the interaction between pavement layers and the impact of geogrid reinforcement. In this study, 12 cyclic triaxial tests on both unreinforced samples and geogrid-reinforced with 3 different geogrids. The tests were aiming to explore the roles of geogrid placement and type of improving the mechanical behavior of the pavement.

2 METHODOLOGY

The cyclic triaxial (CT) test is a laboratory test used to evaluate the behavior of soils under repeated loading and unloading conditions, which represent traffic loading. The test involves subjecting a cylindrical soil sample to a series of cyclic axial and radial (confining) stresses while measuring the resulting deformation and strength properties. Each soil sample measures 150 mm (6 inches) in diameter and 300 mm (12 inches) in height. The lower part of the sample contains the subgrade material (clay-sand mix), and the upper part contains the aggregate material (57% of sub-ballast and 43% of 57" gravel), which represents the base course. In control samples, the aggregate base is directly compacted on top of the subgrade. In reinforced samples, a circular geogrid sample 150 mm (6 inches) in diameter is placed in between the two materials, where the aggregate is compacted on top of the geogrid. All materials are compacted within a rubber membrane held in place by a vacuumed mold. The sample is secured via two O-rings at the top and bottom. The sample is then transferred to the triaxial chamber, and a cell pressure is applied. The vacuum could be released at this time. Figure 1 shows different features of the CT equipment and sample preparation.

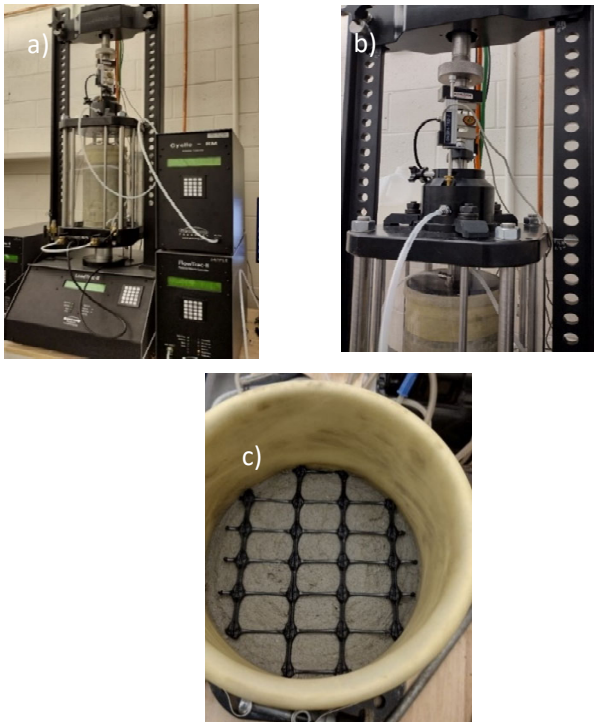

Figure 1. a) Cyclic triaxial setup, b) Dynamic actuator, c) Geogrid sample placed on top of the Subgrade

The sample is instrumented with two Linear Variable Differential Transducers (LVDTs) located on top of the triaxial chamber; the calculations use an average of the two values. A loading sequence is programmed into the CT machine to apply variable confining and axial stresses following the guidance of AASHTO T 307 procedure 8 .

The total CT testing program consists of thirty tests, including three CBR samples, unreinforced control samples, and three geogrids: 3D Grid 1, 3D Grid 2 and 3D Grid 3 reinforced samples. Each sample is tested with a subgrade CBR of 1%, 2%, and 4% and an aggregate base thickness of 50 mm, 100 mm, and 200 mm (2 in, 4 in, and 8 in). In this paper, the results of only 12 tests are presented for the samples with 50 mm base thickness.

The load cycle total duration is 1.0 second; each consists of a max stress that lasts 0.2 seconds, followed by a contact stress for 0.8 seconds. Each loading sequence is repeated for a predetermined maximum number of load applications or cycles. Each loading sequence terminates and moves to the following sequence when either the maximum number of cycles or a total strain of 5% is reached. The maximum applied stress is experienced by the sample during the initial 0.2 seconds of the loading cycle duration. Conversely, the contact stress pertains to the stress endured within the subsequent 0.8-second period. The difference between the maximum stress and the contact stress represents the applied cyclic stress S_{cyclic}. Figure 2 shows the variation in load within a typical loading cycle. Upon the release of the cyclic stress S_{cyclic}, the CT machine software differentiates between the plastic strain (ε_p) within the sample and the elastic

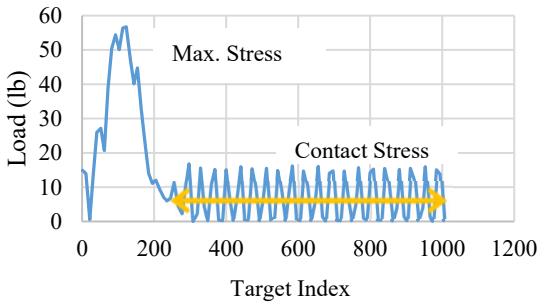

Figure 2 Variation in load within a typical loading cycle

strain (ε_r). The Resilient Modulus (M_R) is calculated by dividing the cyclic stress (S_{cyclic}) by the elastic strain (ε_r).

3 MATERIALS

3.1 *Subgrade*

The material that was used in the CT tests to represent the subgrade under the roadway section is a mixture of 40% clay and 60% sand. The clay used is sodium Bentonite 325 with Liquid Limit (LL) of 617% and Plastic Index (PI) of 445%. The sand is silica sand which maintains particle size between 0.425 and 0.85 mm (US sieve 20 -40).

3.2 *California Bearing Ratio CBR*

The clay-sand mixture was mixed with different moisture contents to obtain a particular CBR strength, and a CBR test (ASTM D1883) was performed on the sample Table. 5. A relationship between the CBR and moisture content was obtained as shown in Figure 3.

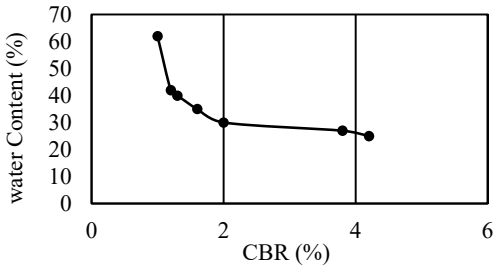

Figure 3. CBR V/s water content

3.3 *Aggregate Base*

An aggregate base is a layer of granular material placed on top of a pavement's subgrade or subbase. To represent this layer and to match it with a grain size distribution that was used previously in another geogrid testing (Target), two materials; granite #57 and sub-ballast granite were mixed with 43% and 57%, respectively. Figure 4 shows the grain size distribution of the three materials.

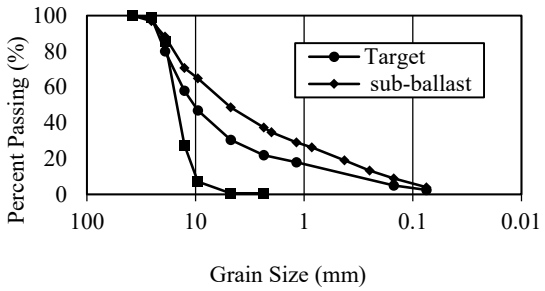

Figure 4. Grain size distribution of aggregate base

3.4 *Moisture-density relationship*

To achieve a target density that is consistent throughout the tests, a modified compaction test (ASTM D1556) was performed on the aggregate base as shown in Figure 5. The aggregate used in the CT tests was compacted to a density that ranged between 22 to 24 kN/m^3 (137 to 143 pcf) and a target moisture content of 6%. At least 90% of modified compaction was achieved.

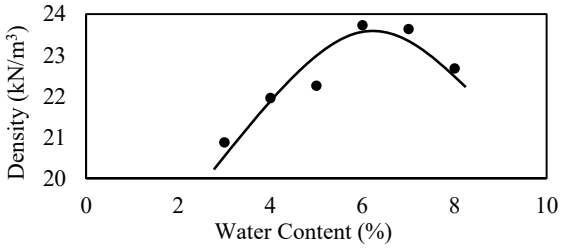

Figure 5. Modified compaction curve (ASTM D1556) of aggregate base

3.5 *Geogrids*

Geogrids are polymeric products designed to improve the performance of subgrade soils by distributing loads more evenly and increasing the subgrade soil's resistance to deformation and rutting. The primary mechanism of such improvement is lateral confinement along the main deformation direction. Other mechanisms include improvement of bearing capacity and membrane effect. Three types of geogrids investigated in this research study; 3D Grid 1, 2 and 3. Figure 6 shows a picture of the three geogrids. Table 1 presents the physical dimensions measured with a caliber in machine direction (MD) and cross-machine direction (XD), in addition to the soil- geosynthetic composite stiffness of each geogrid.

4 RESULTS AND ANALYSIS

4.1 *Cyclic Triaxial (CT) Data Analysis*

The CT software records the applied load for each loading cycle and the associated deformation on top of the sample. The data is then converted to a comma separated value (csv) file where further calculations of the data are warranted so that maximum stress, contact stress, elastic strain and plastic strain are determined.

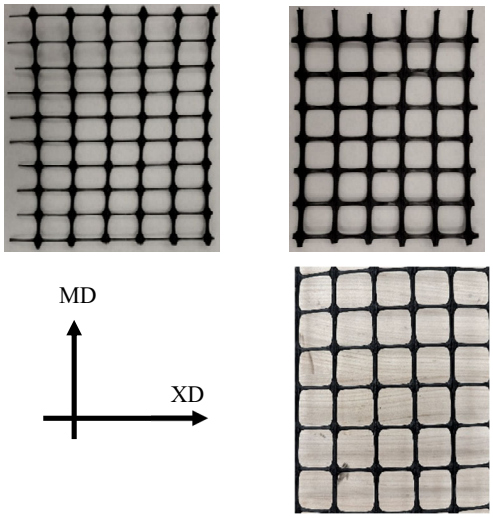

Figure 6. a. 3D *G*rid 1, b. 3D Grid 2, c. 3D Grid 3

Table 1. Physical and mechanical properties of geogrids

Description	3D Grid 1	3D Grid 2	3D Grid 3
MD opening size (mm)	24	31	32
XD opening size (mm)	34	32.5	32
MD rib width (mm)	3.0	4.0	3.5
XD rib width (mm)	1.3	3.5	1.2
MD rib thickness (mm)	2.5	3.5	3.7
XD rib thickness (mm)	0.5	1.0	2.0
Joint thickness (mm)	6.0	5.5	4.5
Soil-Geosynthetic composite stiffness (kN/m)^2/mm	30	32	38

Initially, the load data are refined by removing a calibrated offset and then multiplying by a calibrated factor to obtain the final load (Lf), ensuring measurement accuracy. Similarly, for displacements, initial readings are subtracted to zero at the start of the cycle, and a factor is applied to determine the actual displacements experienced by the sample (Df1, Df2). Following these adjustments, the average displacement from both sensors is calculated and converted into plastic strain to assess the soil sample's deformation relative to its original size.

The analysis involves identifying the maximum total strain and average plastic strain in each loading cycle to determine the extent of deformation. The elastic strain is then calculated by subtracting the average plastic strain from the maximum total strain, indicating the soil's recovery ability after stress. The resilient modulus, reflecting soil elasticity, is derived by dividing cyclic stress S_{cyclic} by the elastic strain.

4.2 *Plastic Strain Formulation*

The plastic behavior of materials under stress is a critical aspect in engineering and materials science. Understanding how plastic strain evolves with stress conditions is essential for design, safety, and reliability. Several research studies have documented the relationships between plastic deformation characteristics,

experimental variables, and fundamental soil properties. Some of the limitations of these empirical equations involve not separating the effect of confining stress from that of the deviator stress or including just the axial stress. Therefore, in this study, a model including parameters that can independently account for the effects of confining stress, deviator stress on plastic strain is adopted. A four-parameter cyclic composite model is used to formulate the plastic strain. In this formulation, normalized octahedral normal stress σ_{oct}, normalized octahedral shear stress τ_{oct}, and the number of loading cycles *N* are considered as the influencing factors in the plastic strain. The formulation for triaxial type loading conditions is presented in Equation 1 (Puppala et al., 2009).

$$\varepsilon_p = \propto_1 . N^{\propto_2} . \left(\frac{\sigma_{oct}}{\sigma_{atm}}\right)^{\propto_3} . \left(\frac{\tau_{oct}}{\sigma_{atm}}\right)^{\propto_4} \quad (1)$$

where $\sigma_{oct} = \frac{(\sigma_1 + 2\,\sigma_3)}{3}$, $\tau_{oct} = \frac{\sqrt{2}}{3} . (\sigma_1 - \sigma_3)$, σ_1 is the axial stress, σ_3 is the confinement stress, $\sigma_1 - \sigma_3$ = deviator stress, σ_{atm} is the standard atmospheric pressure at the sea level which is approximately 101.3 kPa and *N* = number of loading cycles. α_1, α_2, α_3, α_4 are the cyclic composite model constraints that play a crucial role in capturing the behavior of plastic deformation in the sample under repetitive loading.

4.3 *Resilient Modulus (M_R)*

The resilient modulus reflects how soil or granular materials respond to stress by considering recoverable strain (elastic strain), different from the modulus of elasticity, which considers total strain. Resilient modulus excludes permanent deformation, focusing solely on elasticity. The test protocol, standardized under AASHTO T-274, seeks to replicate the behavior of pavement materials under repeated traffic loading, mimicking real-world conditions as closely as possible. Elliott et al., 1988 indicated that one of the critical parameters in pavement design is the subgrade soil's resilient modulus (M_R). As vehicles traverse the pavement, the pavement layers react to the repeated loading. Deformation behavior under a repeated load test is illustrated in Figure 7. Significant permanent deformation, denoted as plastic strain. With an increase in load repetitions, the plastic strain from each load repetition diminishes. After numerous repetitions, the strain becomes recoverable. The resilient modulus, denoted as M_R, is the elastic modulus determined based on the recoverable strain under repeated loads. M_R is calculated as the ratio of applied deviator stress (σ_d) to recoverable or elastic strain (ε_r), Carmichael and Stuart, 1985. M_R ratio is percent increase or decrease compared to the control section

5 DISCUSSION

5.1 *Resilient Modulus*

The results acquired from the CT testing and further analyses revealed that including 3D geogrids significantly enhanced the combined resilient modulus for most of the cases across different

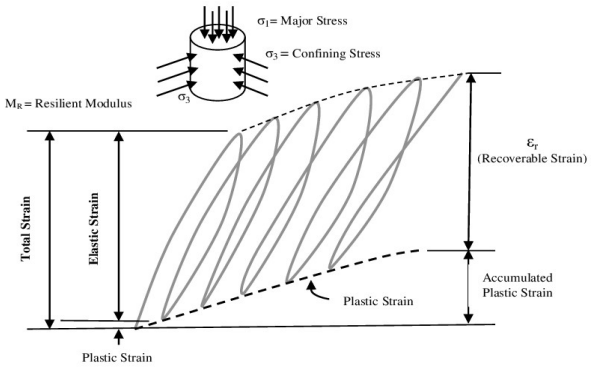

Figure 7. Plastic and elastic strain response for cyclic loading (after Sadrossadat et al., 2016)

subgrade strength or CBR values when compared to control (unreinforced) sections. for 3D Grid 1, the resilient modulus increased by 24%, 58% and decreased by 8% for subgrade CBR of 1%, 2 % and 4%, respectively. For 3D Grid 2, the resilient modulus increased by 26 %, 64 %, and decreased by 24 %, for subgrade CBR of 1%, 2 % and 4%, respectively. For 3D Grid 3, the resilient modulus decreased by 11%, increased by 190%, and decreased by 52%, for subgrade CBR of 1%, 2 % and 4%, respectively. Table 2 shows the results of the cyclic triaxial tests.

Table 2. Cyclic triaxial test results

Test #	CBR (%)	Resilient Strain (%)	Permanent Strain (%)	Resilient Modulus M_R (kPa)	M_R Ratio (%)
Control	1	0.48	4.19	5754	
Grid 1	1	0.38	1.22	7134	24
Grid 2	1	0.37	1.09	7258	26
Grid 3*	1	0.71	4.09	5077	-11
Control	2	0.34	1.81	11733	
Grid 1	2	0.15	0.96	18580	58
Grid 2	2	0.14	0.91	19295	64
Grid 3*	2	0.10	1.21	33945	190
Control	4	0.07	0.27	33318	
Grid 1	4	0.08	0.33	30631	-8
Grid 2	4	0.10	0.33	25167	-24
Grid 3*	4	0.07	0.75	50595	52

*higher deviator stress loading sequence

The variation in resilient modulus, with specific sections and testing conditions showing a drop and others an increase, is influenced by the subgrade strength, normal and deviator stresses, and geogrid properties, which all determine the level by which the geogrid strength is mobilized to provide base reinforcement. An ideal combination of a subgrade strength and deviator stress under the testing conditions, mobilizes the geogrid to exhibit an optimal reinforcement benefit. This could be shown by the percent increase in M_R of 58%, 64% and 190%, for 3D Grid 1, 2 and 3, respectively, at CBR of 2. The cases with

decrease in the M_R value occurred when higher stresses could not be reached to mobilize the geogrid strength.

5.2 *Permanent strain*

The specific design and material properties of the geogrids can lead to varied performance improvements at different testing conditions. When comparing the performance of 3D Grid 1, 3D Grid 2 and 3D Grid 3 based on plastic or permanent strain results, the three geogrids demonstrate improvement in soil performance compared to control tests. The performance varies depending on the specific test loading sequence, CBR values, or subgrade strength and base thickness. The 3D Grid 2 shows a lower plastic strain in most tests, which suggests better long-term rutting resistance. On the other hand, the 3D Grid 1 occasionally achieves a higher resilient modulus, indicating improved elasticity and load recovery ability in specific sequences. The 3D Grid 3 shows lower plastic strain consistently.

At a CBR of 1%, 3D Grid 1, 3D Grid 2 and 3D Grid 3 reduce the total and plastic strain compared to the control section. 3D Grid 2 often results in a slightly lower plastic strain, indicating better performance in minimizing irreversible deformation. At higher CBR values, such as 4% with the same base depth, the trend continues with 3D Grid 2 providing lower plastic strain but with some exceptions where the 3D Grid 1 performs better in terms of resilient modulus. The better performance of the 3D Grid 2 in terms of plastic strain could be attributed to its enhanced interlocking capabilities, allowing for more effective load distribution and less deformation.

5.3 *Base Thickness*

The base thickness required to support given wheel load is calculated by incorporating the normal stress (σ_z) distributed at various depths (z) using Equation 2. The plastic strain calculation is based on Equation 1 considering the model constraints: α_1, α_2, α_3, α_4 for each condition, normal and shear stress. The calculation of deformation at each assumed base thickness allowed for the determination of the design thickness based on the allowable ruth depth criteria.

$$\sigma_z = 0.84p\left(1 - \frac{z^3}{(bl+z^2)^{1.5}}\right) \quad (2)$$

The geogrid materials, 3D Grid 1, 3D Grid 2 and 3D Grid 3, are uniquely designed for specific purposes in stabilizing soil and constructing roads. 3D Grid 1 has smaller center-to-center openings of 24 mm by 34 mm, making it suitable for moderate loads and emphasizing aggregate interlock. The ribs are 3 mm wide, which offers a balance between strength and flexibility. On the other hand, 3D Grid 2 has more of a square opening of 31 mm by 32.5 mm, with robust ribs that enhance resilience and deformation resistance. The thickness of the rib underscores their strength and load-bearing capabilities, and heavier-duty applications. 3D Grid 3 has a larger square opening 32.0 mm by 32.0 mm, making it suitable for heavy loads and equal interlocking behavior in MD and XD directions. With its thick XD rib of 2 mm, which gives it the ability to significantly improve the resilient modulus at higher CBR values.

6 CONCLUSIONS

In this research study, a comprehensive cyclic triaxial (CT) testing program was performed consisting of 12 composite samples. The 12 samples consisted of 4 sets of samples: unreinforced/ control, and reinforced by 3D Grid 1, 3D Grid 2, and 3D Grid 3. Each of the 4 seta were tested at 3 subgrade CBR values, 1%, 2% and 4%. The cyclic loading was applied to the composite samples to assess pavement structure performance under simulated traffic loads. The testing process aims to measure total deformation and stress response replicating road conditions. Deformations are further analyzed to distinguish between elastic and plastic strains. This allows the evaluation of the material's recovery capability, indicated by the Resilient Modulus (M_R), and irrecoverable plastic strains.

The samples measured 150 mm in diameter and 300 mm in height. The tests were run under different loading sequences ranging from 41 kPa to 55 kPa (6 psi to 8 psi) of confining stress and deviatoric stress from 13.7 kPa to 124 kPa (2 psi to 18 psi). The loading sequences were run for different numbers of cycles ranging from 500 to 50,000 per sequence. Each load cycle lasted one second (1 Hz), within this one-second cycle, the maximum stress was applied for the initial 0.2 seconds, followed by a contact stress phase lasting 0.8 seconds. The contact stress was set at 10% of the maximum stress value. Both unreinforced and geogrid- reinforced samples were included in the testing program to assess the effect of geogrids on soil strength and resilience.

The analysis on the CT test results was performed using MATLAB to compute the stress and strain parameters and resilient modulus (M_R) from raw data. The data collected from the CT software was stored in CSV files. The analysis involved identifying the total, elastic, and plastic strain in each loading cycle. The cyclic composite model constraints α1, α2, α3, α4 used in unpaved roadway design to predict base thickness for unreinforced and reinforced sections based on a limiting rutting depth.

The Resilient Modulus (M_R) values were calculated using elastic strain and cyclic stress. Tests showed that geogrid-reinforced sections exhibited a higher M_R than the control in most of the cases. Due to the testing limitations and loading sequences that did not quite mobilize the tensile strength in the geogrids, some tests showed a reverse behavior. In general, geogrid reinforcement was observed to enhance base layer performance under higher mobilization conditions, such as at lower subgrade CBR, or higher deviatoric stress. The results indicated the benefits of incorporating geogrids in pavement design for optimal load-bearing capacity.

The physical properties of 3D Grid 2 and 3D Grid 3 featured apertures smaller than 3D Grid 1 in the cross-machine direction, facilitating enhanced interlocking with the aggregate. Also, the rib thickness of 3D Grid 2 and 3D Grid 3 was higher than that of 3D Grid 1, indicating potential improvements in performance due to lateral constraint. To assess the benefit of geogrid reinforcement, the base thickness for 3D Grid 1, 3D Grid 2, and

3D Grid 3 reinforced pavement section was estimated using the cyclic composite model and associated constraints: α1, α2, α3, α4. Given a rutting depth based on permanent strain, a reduction factor that quantifies the base thickness saved when geogrid reinforcement is calculated. The reduction factor for 3D Grid 1 ranged between 35 % to 83 %, for 3D Grid 2 ranged between 40 to 86%, and for 3D grid 3 ranged between 36 % to 90 %. With the increase in wheel load, the reduction factor decreases; however, it increases with an increase in CBR where a lower base thickness under the same wheel load causes a higher level of geogrid mobilized confinement.

7 REFERENCES

American Association of State Highway and Transportation Officials 2021. AASHTO T 307 "Standard Method of Test for Determining the Resilient Modulus of Soils and Aggregate Materials."

AL Sa'adi, A. H. M., Al-Khafaji, F. F., Hashim, T. M., Hussein, M. L. A., Ali, Y. A., Ali, A. H., Jebur, Y. M., Ali, L. H., Al-Mulali, M. Z., & Al-Khazraji, A. A. 2022. The prospect of using geotextile reinforcement within flexible pavement layers to reduce the effects of rutting in the middle and southern parts of Iraq. *Journal of Mechanical Behaviour of Materials*, *31*(1), 323–336. https://doi.org/10.1515/jmbm-2022-0040

Carmichael, R. F. III and Stuart, E. 1985. Predicting resilient modulus: A study to determine the mechanical properties of subgrade soils. Transportation Research Record, No 1043, Transportation Research Board, National Research Council, pp. 145-148

Elliott, R. P., & Thornton, S. I. 1988. Resilient modulus and AASHTO pavement design. *Transportation research record*, (1196).

Ellithy, G. S., & Crippa, A. 2023. Quantifying geogrid reinforcement mechanism in roadway performance using Cyclic Plate Load (CPL) test. 12th International Conference on Geosynthetics, 17-21 Sep, Rome, Italy.

Kiptoo, D., Aschrafi, J., Kalumba, D., Lehn, J., Moormann, C., & Zannoni, E. 2017. Laboratory Investigation of a Geosynthetic Reinforced Pavement Under Static and Dynamic Loading. *Journal of Testing and Evaluation*, *45*(1), 76–84. https://doi.org/10.1520/JTE20160170

Puppala, A. J., Saride, S., & Chomtid, S. 2009. Experimental and modeling studies of permanent strains of subgrade soils. Journal of geotechnical and geo-environmental engineering, 135(10), 1379-1389).

Salama, A., Elboudy, A., & Saleh, N. 2023. Evaluation of Geogrid in Unpaved Road Constructed on Sand Subgrade under Cyclic Loading. *Delta University Scientific Journal*, *6*(1), 103–110. https://doi.org/10.21608/dusj.2023.291018

Sadrossadat, E., Heidaripanah, A., & Ghorbani, B. 2016. Towards application of linear genetic programming for indirect estimation of the resilient modulus of pavements subgrade soils. Road Materials and Pavement Design, 1-15.

Singh, A. K., & Sahoo, J. P. 2021. Rutting prediction models for flexible pavement structures: A review of historical and recent developments. *Journal of Traffic and Transportation Engineering (English Edition)*, *8*(3), 315–338. https://doi.org/10.1016/j.jtte.2021.04.003

Wang, J., Cai, Y., & Yang, F. 2013. Effects of Initial Shear Stress on Cyclic Behavior of Saturated Soft Clay. *Marine Georesources & Geotechnology*, *31*(1), 86–106. https://doi.org/10.1080/1064119X.2012.676153

Ziaie Moayed, R., & Alibolandi, M. 2018. Effect of geotextile reinforcement on cyclic undrained behavior of sand. *Soil Dynamics and Earthquake Engineering (1984)*, *104*, 395–402. https://doi.org/10.1016/j.soildyn.2017.11.013